

# Challenges and Solutions in the Protection of a Long Line in the Furnas System

Ricardo Abboud

*Schweitzer Engineering Laboratories, Inc.*

Walmer Ferreira Soares and Fernando Goldman

*Furnas Centrais Elébricas S.A.*

Presented at the  
DistribuTECH Conference  
Tampa, Florida  
February 7–9, 2006

Previous revised edition released November 2005

Originally presented at the  
32nd Annual Western Protective Relay Conference, October 2005

# Challenges and Solutions in the Protection of a Long Line in the Furnas System

Ricardo Abboud, *Schweitzer Engineering Laboratories, Inc.*  
 Walmer Ferreira Soares, *Furnas Centrais Elétricas S.A. – Brazil*  
 Fernando Goldman, *Furnas Centrais Elétricas S.A. – Brazil*

**Abstract**—In recent years, the use of modern numerical relays for high and extra-high voltage transmission line protection has greatly simplified the job of engineers and technicians involved in the planning, development, design, implementation and commissioning of power system installations.

The great number of features and applications available within each numerical relay, as well as the flexibility of implementing the settings with these devices make their use much easier compared to early electromechanical and static relays. Power system engineers and technicians today have great flexibility in how they apply various protection features. They can select from various protection setting groups within digital protective relays to match the operational philosophy of entire protection schemes.

Despite this apparent ease of application, transmission line protection is still one of the more challenging areas in power system engineering. Selecting the appropriate relays to apply and determining how best to use all available relay features are crucial for correct power system performance.

Some transmission lines have characteristics so distinct and complex that they represent true challenges for even the most advanced relays and most experienced protection professionals. The Ouro Preto 2 – Vitória 345 kV Transmission Line, which runs about 382 km between the substations of two different Brazilian utilities, is one of these challenges.

This paper shows the several challenges, from basic definitions to final line tests, that protection personnel addressed in the power system protection design for the Ouro Preto 2 - Vitória Transmission Line. The paper describes the technical difficulties these personnel encountered when defining line protection system requirements. These difficulties included low short-circuit current level and high line loading operating conditions in the line, a need for single-pole reclose, high terminal voltages during low or no-load operating condition, a need for insertion of neutral reactors, the required reliability level, and the availability of communications schemes.

The paper also shows how relay choice positively influenced the development of the system design and performance analysis tests, which protection personnel performed through the use of a real-time digital simulator (RTDST<sup>™</sup>).

## I. INTRODUCTION

The Ouro Preto 2 – Vitória 345 kV Transmission Line is about 382 km long and interconnects the substations of two different Brazilian utilities: the Ouro Preto 2 Substation, owned by CEMIG, and the Vitória Substation, owned by Furnas.

Furnas Centrais Eletricas S.A. was responsible for building and operating this transmission line. As Furnas personnel resolved construction, environmental, and legal challenges, they

began to face difficulties concerning definition of the transmission line protection system.

Because this transmission line is unique in the basic network of the national interconnected system, and because loss of the line would require significant network rearrangement and hugely impact the city of Vitória in the state of Espírito Santo, it was critical to have a reliable protection system.

Considering the length of the line and consequent associated shunt capacitance, studies showed that the line needed reactors at both ends. These reactors, switched by circuit breakers, would correspond to 60 MVAR of shunt reactive compensation.

Associated with each reactor bank is a neutral reactor whose function is to reduce the secondary arc during the open phase interval after a single-pole trip.

Because of the importance of the line and associated characteristics as a result of the line length, protection personnel provided the protection system with features that surpass the network procedure requirements of The Brazilian Electrical Power System Agency (“Operador Nacional do Sistema Elétrico” – ONS) and Furnas standards.

## II. DESCRIPTION OF THE LINE PROTECTION SYSTEM

### A. Backup Philosophy

Furnas, the utility responsible for the transmission line, adopted a local backup philosophy for internal faults in its transmission system. In other words, Furnas developed protection of the line to avoid dependence on transmission system remote backup protection.

To better meet the requirements of this philosophy, project protection personnel implemented the following measures:

- Each circuit breaker has two tripping coils supplied by distinct dc sources.
- The transmission line is protected by two completely independent and identical protection schemes, each of which connects to a different dc circuit.
- Each protection scheme will trip both circuit breaker coils.
- The voltage and current information for each protection scheme comes from different current transformer cores and potential transformer secondary windings.
- A specific breaker failure scheme protects each circuit breaker associated with the line. The breaker failure protection scheme is initiated by protection functions that issue the trip command to the circuit breakers.

### B. Redundancy Level Adopted

In addition to employing the previously discussed local backup protection philosophy for lines at this voltage, Furnas uses total redundancy between the two protection schemes so that there are dual primary protection systems. Thus, the line protection system can support failures or loss of components without degradation of performance.

To achieve this redundancy, each Ouro Preto 2 – Vitória Transmission Line terminal has two totally redundant, identical, and independent protection systems, referred to as Primary Protection (Main 1) and Alternate Protection (Main 2). Each system is fully capable of selectively detecting and clearing faults that occur in the transmission line without intentional time delay.

### C. Criteria for Choosing Relays

There is much current discussion about the adoption of identical relays in local backup protection schemes. For transmission lines at the voltages this paper discusses, Furnas uses identical relays from the same manufacturer for both primary and alternate protection schemes. This decision facilitated design, integration, maintenance, studies, operation, and training.

As for the common argument that two identical relays could have the same type of failure, thus eliminating the redundancy effect, note that Furnas used RTDS<sup>TM</sup> equipment to subject the chosen relays to specific performance tests for the protected line. Furnas also required evidence of conformance with international standards, thus minimizing the possibility of failure as a result of some inherent relay problem.

In the Ouro Preto 2 – Vitória 345 kV Transmission Line, Furnas adopted relays with proven reliability and performance.

### D. Line Terminal Bus Configurations

The terminals of the Ouro Preto 2 – Vitória Transmission Line have the following bus arrangements:

- Ouro Preto 2: Breaker-and-a-half Configuration
- Vitória: Ring-bus Configuration

These arrangements involve more than one circuit breaker per line terminal, so current, voltage, and trip circuits for each substation terminal become more elaborate.

### E. Total Fault Clearing Time

Furnas designed the protection schemes it applied in the Ouro Preto 2 – Vitória Transmission Line to individually and independently detect and clear multiphase and single-line-to-ground faults for the full length of the line, tripping almost simultaneously at both line ends within the shortest possible time.

The utility designed the protection system of the Ouro Preto 2 – Vitória 345 kV Transmission Line so that the total fault clearing time did not exceed 100 milliseconds. This clearing time included the circuit breaker opening time of all transmission line terminals, which are specified for a maximum interruption time of two cycles at 60 Hz.

Obviously, this protection scheme design implies the need for communications-assisted protection schemes (teleprotec-

tion) and consideration of the time between when one terminal sends a signal and the opposite terminal receives the signal.

### F. Use of Distance Protection Relays

Pilot protection schemes with directional comparison have been in use for more than 50 years and are popular for line teleprotection schemes. These systems use a channel to send permission signals for tripping (permissive) or to block tripping (blocking) based on determination of fault direction by both terminals. Distance directional units and/or sensitive directional overcurrent units usually determine the fault direction.

Communications-assisted protection schemes (teleprotection) based on distance relays frequently use one of the following logic options [1] [2] [3]:

- Direct underreaching transfer trip (DUTT)
- Permissive underreaching transfer trip (PUTT)
- Permissive overreaching transfer trip (POTT)
- Directional comparison unblocking (DCUB)
- Directional comparison blocking (DCB)

Protection personnel can use the flexibility of modern numeric relays to customize teleprotection schemes for specific applications.

The main advantage of protection pilot schemes with directional comparison is minimum channel requirements. These schemes require only the transmission of a logic signal, 0 or 1, to produce a permissive signal or a blocking signal; a large high-bandwidth channel is not necessary. The difference between a directional comparison scheme for single-pole tripping and a directional comparison scheme for three-pole tripping is the need for phase selection.

Traditional directional comparison schemes are based on a local phase selection decision. Through use of other digital communication techniques, such as relay-to-relay communication [4], one can create variants of traditional schemes where phase selection is also intrinsically compared [5].

Phase selection is difficult during cross-country faults, and such difficulty in performing phase selection is an important, practical consideration when protection schemes use directional comparison systems with single-pole tripping.

### G. Teleprotection Scheme Used

In 345 kV transmission lines that use pilot protection schemes with directional comparison, Furnas uses the POTT scheme as a standard scheme and the DCUB scheme when it is known that an internal fault could affect communications channel operation.

Furnas protection personnel designed both the primary and backup protection schemes of the line to operate through the use of a hybrid teleprotection system with simultaneous and superposed operation of a DUTT scheme and a DCUB scheme with weak source logic (weak infeed).

### H. Reclosing Scheme

Both the primary and backup protection schemes of this transmission line include automatic reclosing schemes. Given that the majority of faults in overhead lines – about 80 percent [6] – are temporary and can be cleared by tripping the trans-

mission line and maintaining the line in non-operational status for a few cycles, successful reclosing for these faults is a strong possibility.

Successful reclosing is beneficial to power system stability, while unsuccessful reclosing can be disastrous. We therefore want to increase chances for successful reclosing and block reclosing any time it might be unsuccessful or unnecessary. The Furnas transmission system implements only one-shot reclosing.

Only high-speed protection should start reclosing schemes. In overloaded electrical systems, high-speed automatic reclosing of a transmission line can significantly improve power system voltage conditions related to power quality.

For a transient fault, the success of three-pole automatic reclosing and the total open time interval necessary for the line reclosing scheme depend on synchronization conditions. Single-pole tripping and reclosing help to increase power system stability and inherently maintain synchronism between the two terminals, because a metallic connection remains in place during an open-pole condition. [5]

### I. Selection of Reclosing Type

Furnas protection personnel designed the protection schemes of the Ouro Preto 2 – Vitória Transmission Line to allow selection of two reclose options: “THREE-POLE-MODE” and “SINGLE-POLE-MODE.”

In the “THREE-POLE” mode, any tripping order that the protection system issues opens all three poles (three-pole tripping) and starts the three-pole reclose.

In the “SINGLE-POLE” mode, both single-pole and three-pole tripping are possible. For single-line-to-ground faults (SLGF), only the pole associated with the faulted phase opens (single-pole tripping) and reclosing for that pole is independently implemented in both terminals; for faults that involve more than one phase, three poles trip and three-pole reclosing begins.

The programming of protection relays on the Ouro Preto 2 – Vitória Transmission Line allows Furnas protection personnel to select reclosing only for SLGF either in “SINGLE-POLE” mode or in “THREE-POLE” mode. Any evolving fault will cause the reclosing logic to go to the lockout state, because there is no three-pole reclose initiation.

Fig. 1 represents the reclosing initiation scheme implemented in the Ouro Preto 2 – Vitória Transmission Line.

### J. Selection of the Circuit Breaker to be Reclosed

Given the line terminal configurations in both substations, i.e., a ring-bus arrangement (Vitória Substation) and breaker-and-a-half arrangement (Ouro Preto 2 Substation), either of the two circuit breakers associated with the transmission line terminal can be enabled to reclose. Through local and remote controls, protection personnel can select the circuit breakers that should reclose automatically or disable the reclosing function.

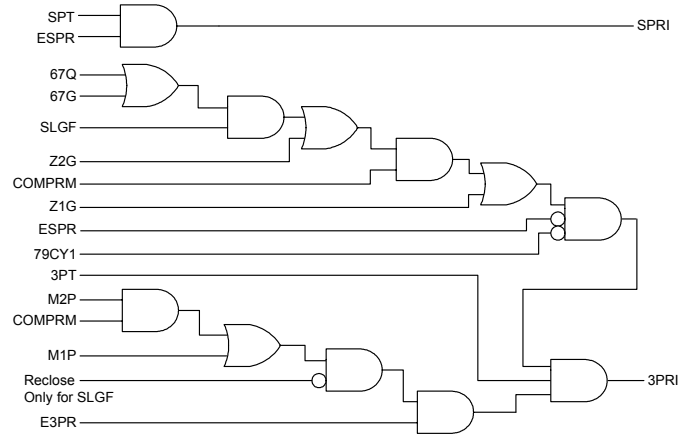


Fig. 1 Reclosing basic logic implemented in the Ouro Preto 2 – Vitória Transmission Line.

Where:

- SPT – Single-Pole Trip
- 3PT – Three-Pole Trip
- ESPR – Single-Pole Reclose Enable
- E3PR – Three-Pole Reclose Enable
- 79CY1 – Relay in Single-Pole Reclose Cycle State
- SLGF – Single-Line-to-Ground Fault
- SPRI – Single-Pole Reclose Initiation
- 3PRI – Three-Pole Reclose Initiation
- 67Q – Sensitive Negative-Sequence Directional Overcurrent
- 67G – Sensitive Zero-Sequence Directional Overcurrent
- Z1G – Zone 1 Ground Distance Element
- Z2G – Zone 2 Ground Distance Element
- M1P – Zone 1 Phase Distance Element
- M2P – Zone 2 Phase Distance Element
- COMPRM – Communications-Assisted Trip Permission

The primary and backup protection relays on the Ouro Preto 2 – Vitória Transmission Line include tools by which protection personnel can configure reclosing features for the two circuit breakers. The reclosing function includes independent timers for setting the open time interval for single-pole and three-pole reclosing cycles.

### K. Single-pole Tripping

Modern numerical line distance relays incorporate single-pole tripping schemes [5]. The inherent benefit of tripping only one pole of the transmission line circuit breakers is that the two substations remain connected by the two other phases, allowing power transfer and reducing the possibility that two line ends lose synchronism.

The use of single-pole tripping followed by single-pole reclosing provides undeniable benefits to system performance. Among the benefits of using single-pole tripping followed by single-pole reclosing are the following:

- Improvement of the stability margin between systems interconnected by the faulted transmission line.
- Minimization of switching surges in the unfaulted phases.

- Improvement of power transmission system reliability and availability during and after a single-line-to-ground fault.

Among the issues one should analyze carefully before choosing the single-pole reclosing option are a relatively long open time interval, with only one circuit breaker pole open; the effect of this open-pole condition on adjacent transmission line protection schemes; and the contribution of unfaulted phases toward maintenance of a secondary arc.

#### L. Main Requirements for Single-Pole Tripping

Obviously, single-pole tripping only makes sense if you intend to initiate single-pole reclosing after the occurrence of a single-line-to-ground fault. In this case, your system must meet such design requirements as the following:

- Circuit breakers should have individual control for each pole.
- The faulted phase selection algorithms should only trip the faulted phase.
- Circuit-breaker pole discrepancy with adjustable time-delays should be coordinated with the single-pole reclosing open time interval.
- Breaker failure schemes should be appropriate for single-pole tripping.

An additional consideration is whether your system needs the addition of neutral reactors to extinguish the secondary arc and allow reduction of the single-pole reclosing open time interval.

### III. TESTS USING RTDS

Analysis of the performance of extra-high voltage (EHV) transmission line protection schemes has become frequent in Brazil. Furnas has adopted a protection system analysis methodology that analyzes each protected item. With this methodology, for example, a company determines if a given relay is effective by taking into account the location in the system where the relay will be applied. To this end, Furnas uses a real-time digital simulator, RTDS, which allows protection personnel to perform a model test with a closed “loop”, illustrated in Fig. 2. To effectively perform fault simulations through use of RTDS, one must follow some steps to validate the model and make the system representation as close as possible to reality.

The first step consists of defining the study area. This study, for example, encompassed the Ouro Preto – Vitória 345 kV Transmission Line, all adjacent lines, the transfer impedances ( $Z_T$ ) between terminals, and the system equivalent sources. Fig. 3 shows the study area.

After defining the study area, we obtained the physical parameters representing the line to be studied and used the electromagnetic transient program ATPDraw to model and calculate line impedances.

After modeling the Ouro Preto 2 - Vitória Transmission Line, we compared the line impedance the program calculated to values the Furnas planning team had calculated previously and found differences in these values. These differences resulted from our use of a correction factor that takes into ac-

count line parameter distortion as a result of line length. A detailed discussion of this factor appears later in this paper.

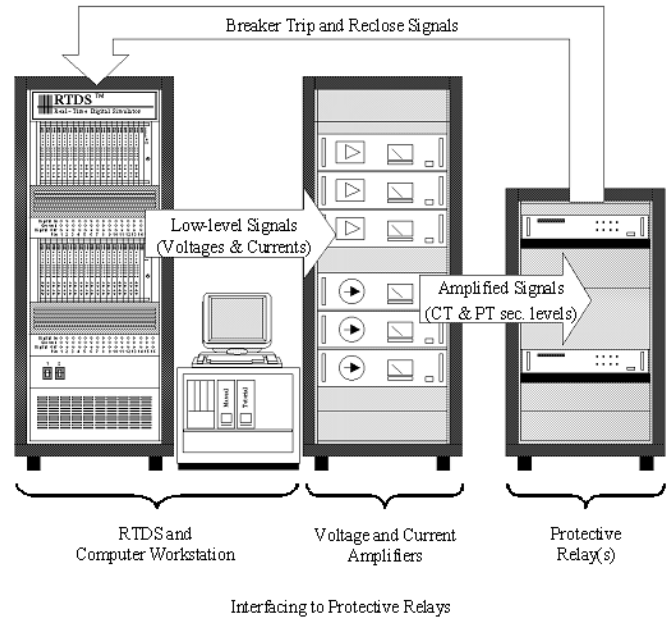


Fig. 2 Test system.

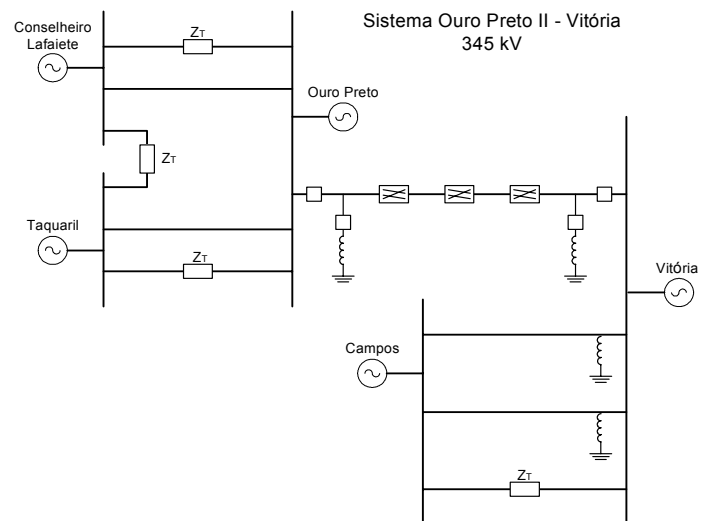


Fig. 3 Ouro Preto 2 - Vitória system study area.

Despite an initial indication regarding two load configurations (light loading and heavy loading), we determined that little variation existed and chose to test only the heavy load condition. For this case, the relays were connected to the RTDS through a digital and analog interface. The relays received current and voltage signals from the simulation. The RTDS received relay digital output signals, including trip signals, and used these signals to control modeled circuit breakers.

Tests consisted of simulated faults at several system locations. Simulations included single-line-to-ground, phase-to-phase, phase-to-phase-to-ground, and three-phase faults. These simulations included faults with and without resistance and with an incidence angle of 0 and 90 electrical degrees (referenced to the faulted phase voltage). The tests also included simulations of evolving faults, reclosing onto fault, and

simulations with and without switching line reactors. Fig. 4 shows the fault locations in the model. P1 and P9 were external, P2 and P8 were in front of the breaker, P3, P4, P5, P6 and P7 were located 10 km, 62 km, 190 km, 320 km, and 372 km from the Ouro Preto terminal.

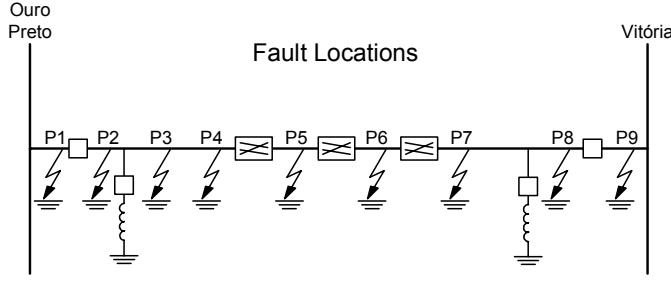


Fig. 4 Fault point locations.

The simulations occurred automatically according to previous programming of the RTDS. Disturbances appeared on the system, and the relays received signals in real time, interacting with the simulation. In the simulation, relay operation issued tripping signals to circuit breakers, dynamically changing system behavior to exactly represent true performance of the evaluated systems.

#### IV. CHALLENGES AND SOLUTIONS FOR PROTECTING A LONG LINE

##### A. The Effect of Fault Resistance

###### 1) The Effect of Fault Resistance in a Radial Line

The effect of fault resistance is to reduce the sensitivity of protection schemes in detecting faults. Fault resistance reduces fault current magnitude and voltage sag in the faulted phase. For single-line-to-ground-faults, fault resistance includes the following components [6]:

- Arc resistance
- Tower resistance
- Tower footing resistance
- Ground return path

Ground faults can also involve such objects as trees, in which case ground fault resistance can reach hundreds of ohms.

Reference [6] indicates that Equation 1 can express arc resistance:

$$R_{Arc} = \frac{440 \cdot l}{I} \quad (1)$$

Where:

$l$  – Arc length in feet

$I$  – Arc current in Amps

Arc resistance is only one component of total fault resistance and is often not the main factor. From Equation 1, one can see that as current decreases, arc resistance (and, therefore, total fault resistance) increases. Fault resistance, therefore, can become large for faults at the remote end of long radial lines because the fault current can fall to very low values.

Fig. 5 shows the effect fault resistance has on distance element measurements in a radial line. For a fault located at a

distance  $m$  (in per unit of transmission line length), Equation 2 provides the impedance. For simplicity, we disregarded the ground return path.

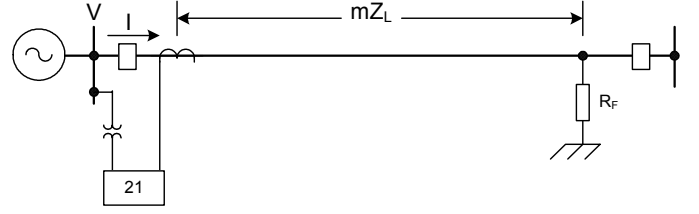


Fig. 5 Fault resistance in a radial line.

$$Z = \frac{V}{I} = mZ_L + R_F \quad (2)$$

In this case, the effect of fault resistance is to add a constant ( $R_F$ ) to the impedance value between the substation and the fault location point ( $mZ_L$ ). Addition of this constant increases the impedance the distance element measures and can cause the distance element to underreach, as Fig. 6 illustrates.

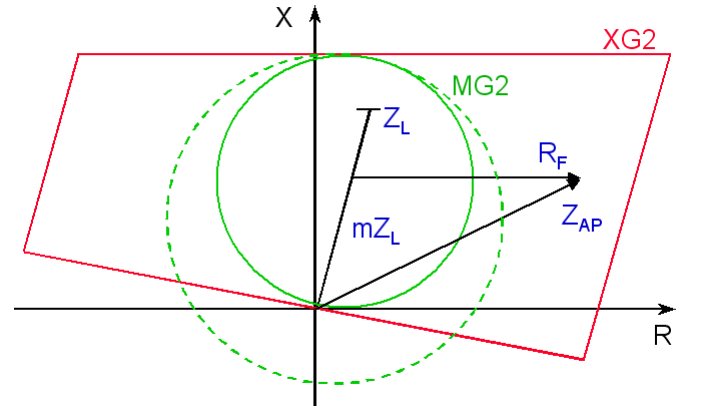


Fig. 6 Effect of fault resistance on the measurement of the distance element.

The positive-sequence memory-polarized mho element expands according to the source impedance (shown by the dashed-line circle in Fig. 6), but distance elements with quadrilateral characteristics can provide greater coverage for  $R_F$  than the mho-type element [7] of Fig. 6, because the resistive reach can be set independently of the reactive reach. It is accepted, however, that the quadrilateral distance element is not a definitive solution for detecting high-impedance faults in transmission lines. Directional sensitive overcurrent elements provide the most sensitive detection of ground faults with high resistance.

###### 2) The Effect of Fault Resistance in a Looped Line

Infeed from the remote source reduces coverage of fault resistance for quadrilateral or mho distance elements. Fig. 7 illustrates the remote source infeed effect. For a fault at a distance  $m$  (in per unit of transmission line length), Equation 3 provides the measured voltage at the relay location. If we divide Equation 3 by Equation 4, we obtain the measured impedance expressed in Equation 5.

$$V = mZ_L(I_S + k_0 3I_{0S}) + I_F R_F \quad (3)$$

$$I = (I_S + k_0 3I_{0S}) \quad (4)$$

$$Z = \frac{V}{I} = mZ_L + \frac{I_F}{I} R_F \quad (5)$$

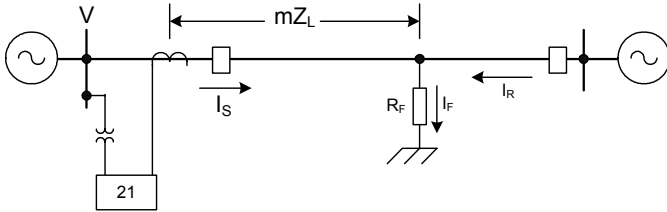


Fig. 7 Fault resistance in a looped line.

The difference between equations 2 and 5 is the  $(I_F/I) \cdot R_F$  term, which is the term related to the remote source infeed. In Fig. 8, we can see that increases in the  $I_F/I$  ratio increase the measured impedance, which causes the distance element to not detect the fault. The  $I_F/I$  ratio increases as the distance from the substation to the fault increases, i.e., the larger the factor  $m$ , the larger the  $I_F/I$  ratio. In long lines, this increased ratio can be very serious because the current,  $I$ , will tend to be much lower than  $I_F$  for faults close to the remote terminal. As a consequence, the apparent impedance will assume high values, and the local terminal will only detect the fault when the remote terminal opens and the infeed current has been removed.

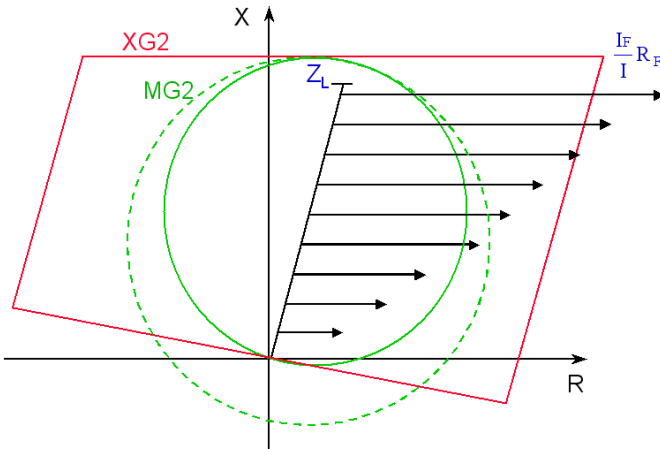


Fig. 8 Effect of fault resistance on distance element measurement, looped line.

Fig. 8, however, is not a good representation of the real infeed effect. The  $(I_F/I) \cdot R_F$  term causes not only an increase in the measured fault resistance magnitude, it also causes a displacement of the measured fault resistance angle [8] [9]. This displacement can be positive or negative, depending on the  $I_F$  and  $I$  angles, and is affected by load flow that causes the measured fault resistance to suffer an angular displacement such as that shown in Fig. 9. For an incoming load condition, the angular displacement is positive (angle shifts upward), and the distance element can underreach. For an outgoing load condition, the angular displacement is negative (angle shifts downward). For inaction in this case, the distance element can overreach.

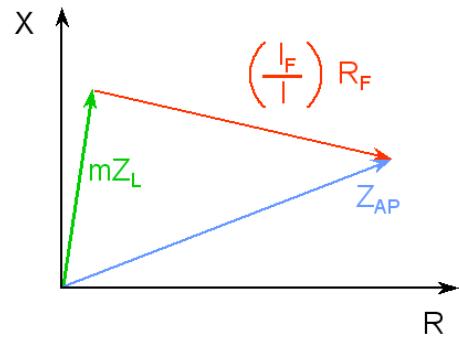
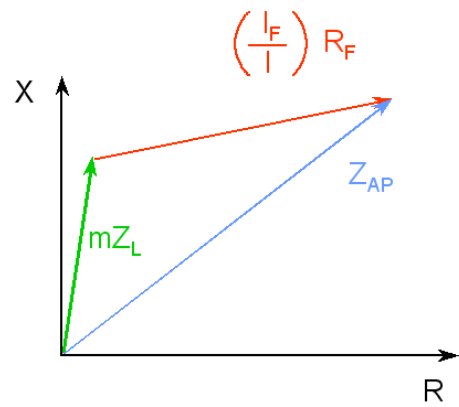


Fig. 9 Effect of fault resistance on distance element measurement, looped line.

### 3) The Effect of Fault Resistance in a Looped Long Line

Furnas uses a sensitive negative-sequence directional over-current element in the directional comparison pilot protection scheme.

As Fig. 10 illustrates, the RTDS provided simulation of a close-in AG fault with a fault resistance of  $100 \Omega$  primary at the Ouro Preto 2 terminal.

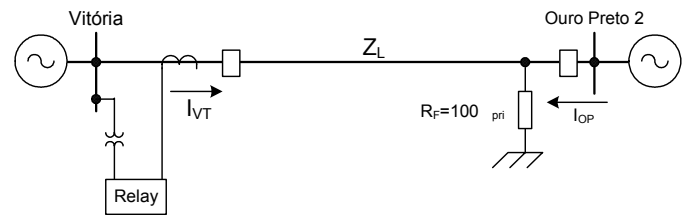


Fig. 10 Close-in fault at Ouro Preto 2,  $R_F=100 \Omega$  primary.

The impedance,  $Z_L$ , is approximately  $140 \Omega$  primary; the adopted value of  $R_F = 100 \Omega$  primary is compatible with values we would expect for EHV transmission lines [6].

In this simulation for heavy load condition real power flow is from the Ouro Preto 2 Substation to the Vitória Substation. Fig. 11 shows an oscillograph we obtained from the Vitória terminal relay that shows the faulted phase current ( $I_{VTA}$ ) and the voltage ( $V_{VTA}$ ) the relay measured during the simulation. In this figure, one can observe that the phase current the Vitória Substation relay measured does not invert direction during fault inception (indicated by the number 1), and the current magnitude decreases, indicating a reduction in power flow and a fault current that is less than load current.

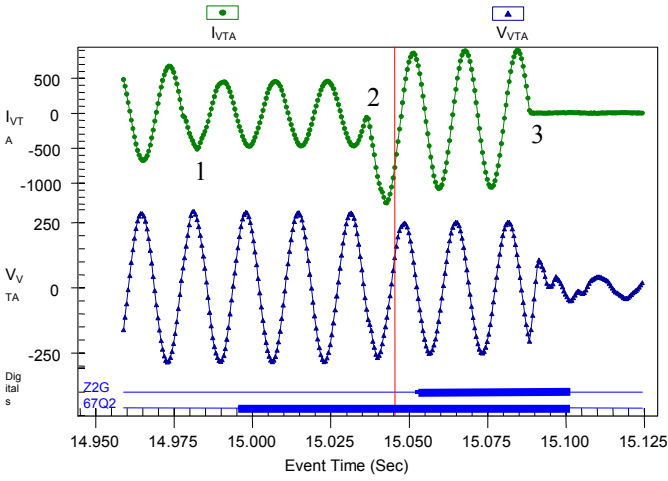


Fig. 11 Faulted phase current and voltage measured by the Vitória Substation relay.

Some milliseconds after fault inception, the sensitive negative-sequence directional overcurrent element (67Q2) asserted, but the distance unit (Z2G) did not assert. Zone 2 operated only after the remote terminal (Ouro Preto 2) opened (number 2 in Fig. 11). As Fig. 11 shows, direction of the faulted phase current changed after the remote terminal opened, indicating that the outfeed phenomenon existed before this terminal opened. Even under this condition, the 67Q2 element operated; the quadrilateral distance element would not operate under this condition even if the resistive reach were set to maximum.

Sensitive directional elements are much more effective for detecting high-impedance faults than are quadrilateral distance elements. It is a good practice to apply sensitive directional element in pilot protection schemes.

Fig. 12 shows the current phasors of the faulted phase at the Ouro Preto 2 Substation ( $I_{OPA}$ ) and the Vitória Substation ( $I_{VTA}$ ), as well as the bus voltage at the Vitória Substation ( $V_{VTA}$ ) for the pre-fault condition. Fig. 13 shows the fault condition with both terminals closed, and one can see in the figure an increase in current magnitude at the Ouro Preto 2 Substation. Fig. 14 shows the fault condition with the Ouro Preto 2 terminal open, and one can see in the figure that the Vitória terminal current inverts its direction under these conditions.

The simulation demonstrates that it is extremely important that a sensitive negative-sequence directional overcurrent element be used with pilot protection schemes, even for long lines.

Furnas designed Ouro Preto 2 – Vitória Transmission Line protection schemes to allow for selection of one of two modes of operation for reclosing: “THREE-POLE-MODE” and “SINGLE-POLE-MODE.” The protective relaying system that this project used allowed single-pole tripping even when the sensitive negative-sequence directional element operated on its own; the fault selection algorithm is not based on distance elements.

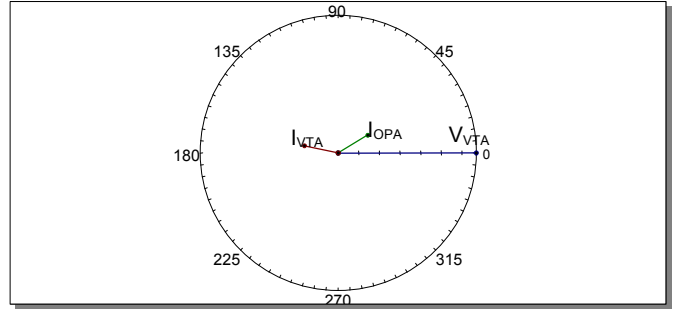


Fig. 12 Pre-fault condition current and voltage phasors.

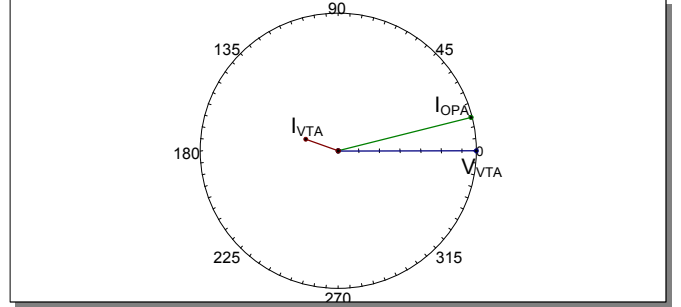


Fig. 13 Current and voltage phasors with both terminals closed.

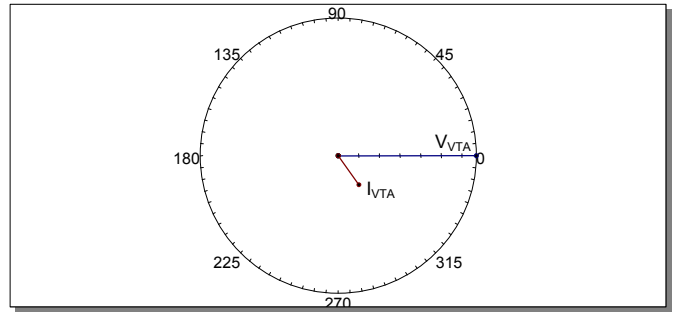


Fig. 14 Current and voltage phasors with the Ouro Preto 2 terminal open.

### B. Heavy Load Condition

Under normal operating conditions, the impedance the phase distance elements measure is the load impedance. The phase distance element measures a low-impedance value for the permanent steady-state condition in lines with high power flow. The measured impedance angle depends on the ratio of reactive power (Q) to real power (P). The lower the Q/P ratio, the lower the measured impedance angle.

$$S \angle \phi = VI \angle \phi = P + jQ \quad (6)$$

$$Z_{LOAD} = \frac{V}{I} \angle \phi = \frac{V^2}{S} \angle \phi \quad (7)$$

During normal heavy load operating conditions, the Q/P ratio remains within certain limits to optimize line power flow.

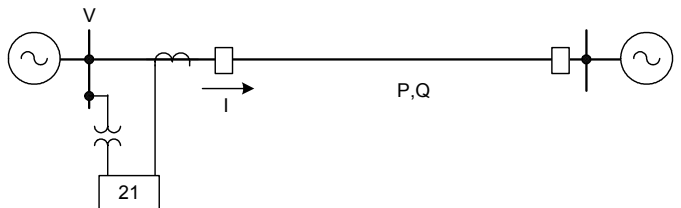


Fig. 15 Power flow in the transmission line.

We can represent the load region in an R-X diagram, as Fig. 16 illustrates.

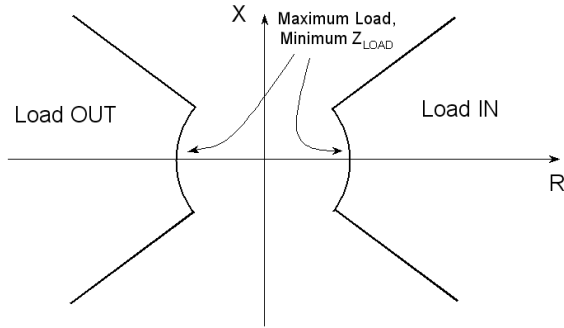


Fig. 16 Load region.

Heavy power flow can cause a problem in long line-distance relay applications, because phase distance elements require long reaches. This requirement could cause the measured phase impedance for the heavy load condition to plot inside the operating region of the distance unit.

Past distance relay implementations used combinations of traditional characteristics to create more appropriate phase distance element operating characteristics for long lines. As an example, Fig. 17 shows two of these characteristics.

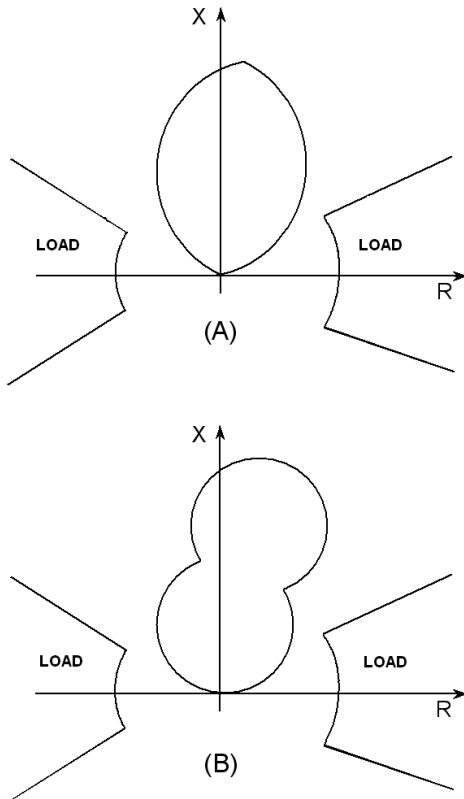


Fig. 17 Traditional distance element operation characteristics used in long lines (A) Lens (B) Peanut.

To prevent phase distance element problems of this kind, one can take advantage of numerical relay features to overlap load and phase distance element characteristics and block phase distance element operation in load regions (load-encroachment characteristic) [9], as Fig. 18 illustrates.

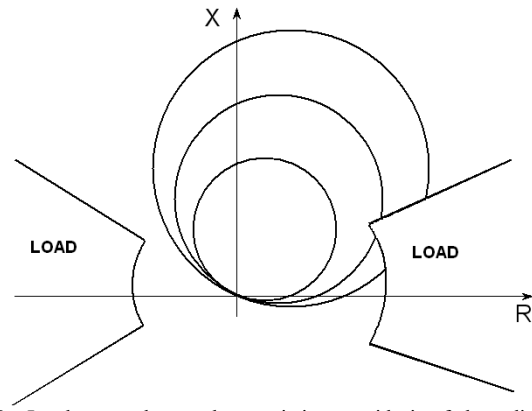


Fig. 18 Load-encroachment characteristic to avoid trip of phase distance element under heavy load.

### C. Ouro Preto 2 – Vitória Transmission Line Parameters

As the Appendix demonstrates, we can use the equivalent  $\pi$  circuit to represent long lines in a permanent steady-state condition. This representation is possible because the impedance  $Z$  and the admittance  $Y$  are corrected by the factors

$$\frac{\sinh \gamma l}{\gamma l} \text{ and } \frac{\tanh \frac{\gamma l}{2}}{\frac{\gamma l}{2}}, \text{ respectively, to provide } Z' \text{ and } Y' \text{ values}$$

according to Equation 8 and Equation 9. These values, that consider long-line characteristics, can then be used in the equivalent  $\pi$  circuit of the transmission line, as Fig. 19 illustrates.

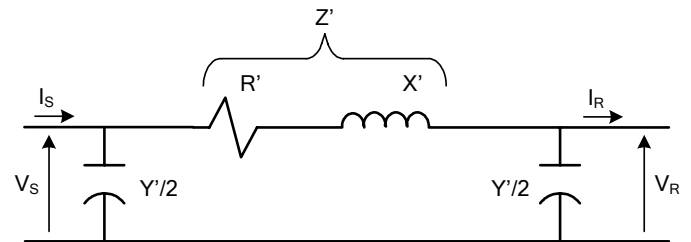


Fig. 19 Long line represented by equivalent  $\pi$  circuit.

$$\frac{Y'}{2} = \frac{Y}{2} \cdot \frac{\tanh \frac{\gamma l}{2}}{\frac{\gamma l}{2}} \quad (8)$$

$$Z' = Z \cdot \frac{\sinh \gamma l}{\gamma l} \quad (9)$$

Where:

$\gamma$  – Propagation constant =  $\sqrt{z \cdot y}$  (1/km)

$l$  – Total line length (km)

$Z$  – Total line impedance =  $R + jX = z \cdot l$  ( $\Omega$ )

$Y$  – Total line admittance =  $G + jB = y \cdot l$  (S)

$Z'$  – Corrected line impedance =  $R' + jX'$  ( $\Omega$ )

$Y'$  – Corrected line admittance =  $G' + jB'$  (S)

$z$  – Line series impedance per unit of length =  $(r+jx)$  ( $\Omega/\text{km}$ )

$y$  – Line shunt admittance per unit of length =  $(g+jb)$  (S/km)

Usually, calculations (rather than measurements) provide EHV transmission line impedance. Considerable data are nec-

essary for the calculation of transmission line parameters. Some values such as cable heights, span lengths, cable sags, and ground resistivity, for example, change for each line span and suggest the use of average values. This ambiguity in line parameter values negatively impacts protection scheme reliability and fault location function, because it introduces unwanted errors.

The parameter values per km of the Ouro Preto 2 – Vitória Transmission Line are as follows:

$$r = 0.034 \Omega/\text{km}$$

$$x = 0.375 \Omega/\text{km}$$

$$g = 0 \text{ S/km}$$

$$b = 4.42 \cdot 10^{-6} \text{ S/km}$$

$$z = 0.034 + j 0.375 \Omega/\text{km}$$

$$y = j 4.42 \cdot 10^{-6} \text{ S/km}$$

$$\gamma = \sqrt{z \cdot y} = 5.828 \cdot 10^{-5} + j 1.288 \cdot 10^{-3} \text{ (1/km)}$$

Where:

$r$  – Line series resistance per unit of length ( $\Omega/\text{km}$ )

$x$  – Line series reactance per unit of length ( $\Omega/\text{km}$ )

$g$  – Line shunt conductance per unit of length (S/km)

$b$  – Line shunt susceptance per unit of length (S/km)

We can use these values to plot the curves in Fig. 20 and visualize the ratios between corrected values of impedance ( $Z' = R' + jX'$ , as per Equation 9) and uncorrected values ( $Z = R + jX$ ).

Note that the distortion is noticeable for line lengths greater than 100 km. There can be a great difference between  $Z$  and  $Z'$  values for long transmission lines.

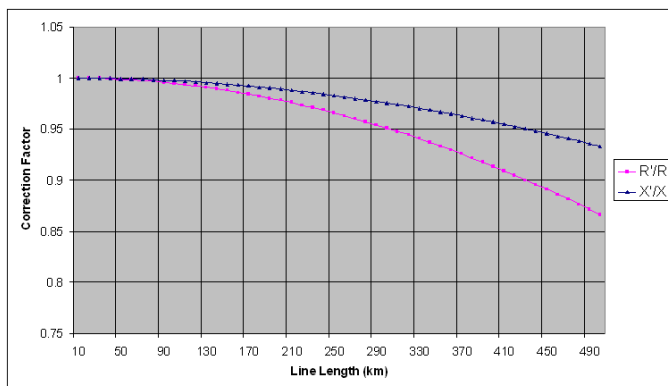


Fig. 20 Ratio between corrected values ( $R'$  and  $X'$ ) and uncorrected values.

In the case of the 382 km-long Ouro Preto 2 – Vitória Transmission Line, values of  $Z$  and  $Z'$  are as follows:

$$Z = z \cdot l = (0.034 + j0.375) \cdot 382$$

$$Z = 12.99 + j143.25 \Omega$$

In polar coordinates, the result is as follows:

$$Z = 143.84 \angle 84.82^\circ$$

From Equation 9, we obtain the following:

$$Z' = (12.99 + j143.25) \cdot \frac{\sinh[(5.828 \cdot 10^{-5} + j1.288 \cdot 10^{-3}) \cdot 382]}{(5.828 \cdot 10^{-5} + j1.288 \cdot 10^{-3}) \cdot 382}$$

$$Z' = 11.96 + j 137.59 \Omega$$

In polar coordinates, the result is as follows:

$$Z' = 138.11 \angle 85.00^\circ \Omega$$

There is a difference of about 4.2 percent between the values of these impedances. This difference can significantly influence fault location and protective relay settings.

Many sources of error, such as a lack of accurate line parameters [10], can influence fault location. In the case of the Ouro Preto 2 – Vitória Transmission Line, a difference of 4.2 percent represents a length of about 17 km. Line impedance measurements can help us determine which impedance values are most correct.

#### a) Measuring the Line Impedance

As the paper mentioned previously, EHV transmission line impedance values are obtained from calculations instead of measurements. The Appendix demonstrates that Equations 8 and 9 correct the impedance of a long line. It would be of great value if we could validate these calculated values.

Modern numerical relays incorporate metering functions that can use to measure impedances of the lines these relays we protect. The relays Furnas used in the Ouro Preto 2 – Vitória Transmission Line incorporate synchronized phasor measurement. Reference [11] provides details about this relay feature that we can use to measure current and voltage phasors of both line ends with the same time reference.

After we powered up the Ouro Preto 2 – Vitória Transmission Line, we measured the line impedance through use of protective relays that provided synchronized phasor measurements. The protective relays of both substations, Ouro Preto 2 and Vitória, connected to the Furnas Engineering Center in Rio de Janeiro through a remote access network such as that illustrated in Fig. 21.

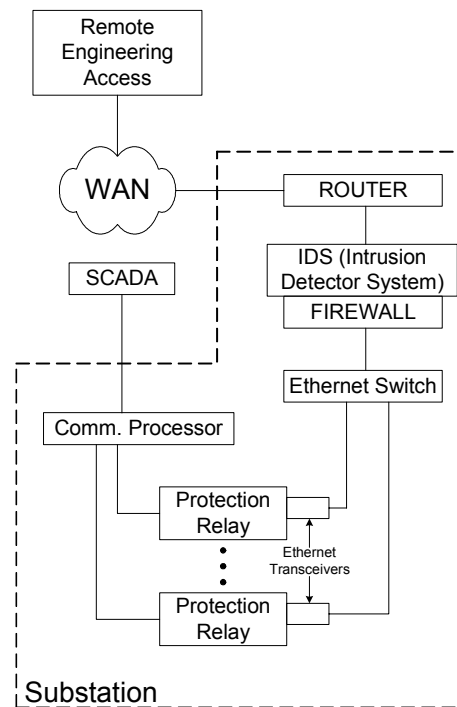


Fig. 21 Remote engineering access.

We had programmed the Ouro Preto 2 and Vitória relays through a remote access network to provide synchronized phasor measurement at a given time. Fig. 22 and Fig. 23, respectively, show the synchronized phasor measurements we obtained from the Ouro Preto 2 and Vitória relays.

The Vitória terminal reactor was connected during the measurement period; so the equivalent circuit is shown in Fig. 24. Let us call the line impedance and admittance we measure through the use of synchronized phasors  $Z_{me}$  and  $Y_{me}$ , respectively.

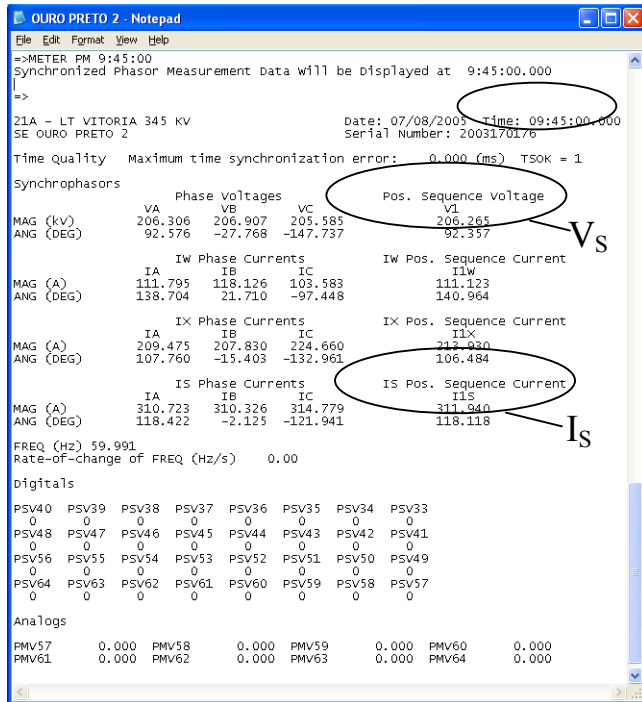


Fig. 22 Synchronized phasor measurement from the relay installed in the Ouro Preto 2 Substation.

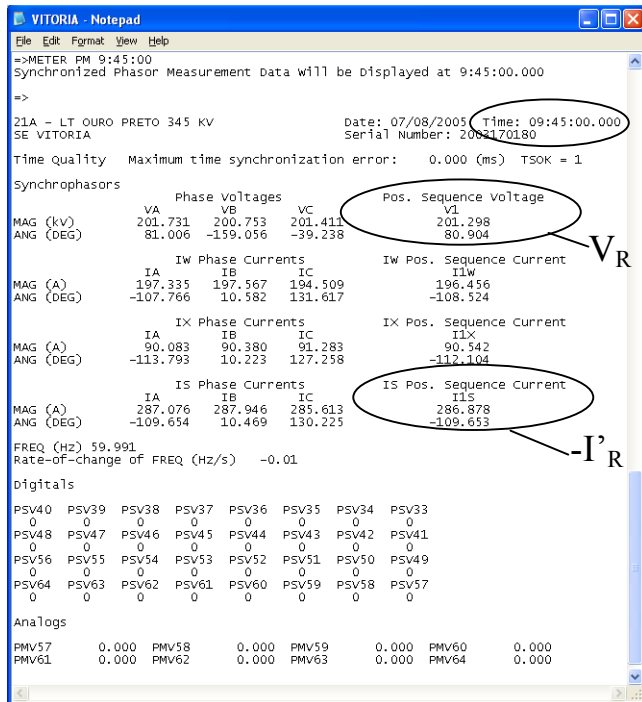


Fig. 23 Synchronized phasor measurement from the relay installed in the Vitória Substation.

According to Fig. 24, the equations that relate the currents and voltages of the Ouro Preto 2 and Vitória terminals with line impedance and admittance are as follows [12]:

$$I_S = V_S \cdot \frac{Y_{me}}{2} + \frac{V_S - V_R}{Z_{me}} \quad (10)$$

$$I_R = \frac{V_S - V_R}{Z_{me}} - V_R \cdot \frac{Y_{me}}{2} \quad (11)$$

Where:

$V_R$  – Voltage at the receiving end (Vitória) of the line (V)

$I_R$  – Current at the receiving end (Vitória) of the line (A)

$V_S$  – Voltage at the sending end (Ouro Preto 2) of the line (V)

$I_S$  – Current at the sending end (Ouro Preto 2) of the line (A)

$Z_{me}$  – Measured total line impedance ( $\Omega$ )

$Y_{me}$  – Measured total line admittance (S)

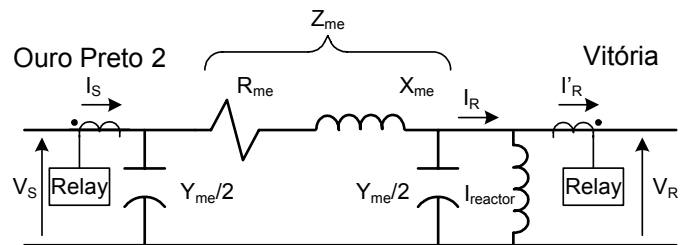


Fig. 24 Equivalent II circuit of the Ouro Preto 2 – Vitória Transmission Line.

When we solve Equation 10 and Equation 11 to find  $Z_{me}$  and  $Y_{me}$  in terms of voltages and currents, we obtain Equation 12 and Equation 13 [12]:

$$Z_{me} = \frac{V_S^2 - V_R^2}{I_S \cdot V_R + I_R \cdot V_S} \quad (12)$$

$$Y_{me} = 2 \cdot \frac{I_S - I_R}{V_S + V_R} \quad (13)$$

To obtain positive-sequence impedance values, we need only to insert the positive-sequence current and voltage values we obtain from synchronized phasor measurement into Equations 12 and 13.

As we can see in Fig. 24, the measured value was the  $I'_R$  current value, not the  $I_R$  value, because the reactor was connected to the Vitória terminal. However, the reactor impedance value is known and we have a measured  $V_R$  voltage, so we can calculate the reactor current,  $I_{reactor}$ , easily at the instant of measurement:

$$I_{reactor} = \frac{V_R}{Z_{reactor}} \quad (14)$$

The  $I_R$  current is according to Equation 15:

$$I_R = I'_R + I_{reactor} = I'_R + \frac{V_R}{Z_{reactor}} \quad (15)$$

Where:

$V_R$  – Positive-sequence voltage measured at the Vitória terminal

$V_S$  – Positive-sequence voltage measured at the Ouro Preto 2 terminal

$I_S$  – Positive-sequence current measured at the Ouro Preto 2 terminal

$I'_R$  – Positive-sequence current measured at the Vitória terminal

$Z_{reactor}$  – Reactor impedance =  $j1,983.79 \Omega$

The current the Vitória terminal relay measures is in phase opposition to  $I'_R$  (Fig. 24), so the measured current was  $-I'_R$ . To obtain  $I'_R$ , we must displace by  $180^\circ$  the positive-sequence current the Vitória terminal measured.

By substituting Equation 15 in Equation 12 and solving for values, we obtain the following:

$$V_S = 206,265 \angle 92.357^\circ \text{ V}$$

$$I_S = 311.940 \angle 118.118^\circ \text{ A}$$

$$V_R = 201,268 \angle 80.904^\circ \text{ V}$$

$$I'_R = 286.878 \angle 70.347^\circ \text{ A}$$

The measured positive-sequence current is as follows:

$$Z_{me} = 144.69 \angle 85.3^\circ \Omega$$

Observe that the measured impedance value,  $Z_{me}$ , is much closer to the impedance  $Z = z \cdot l$  than to the corrected impedance  $Z'$ , which is typically used for protection relay settings and short-circuit studies. We repeated the measurement several times and for different load conditions, but the calculated impedance always was similar to the previous calculated value. The measured impedance is the positive-sequence impedance, which equals negative-sequence impedance for a transmission line.

This measured impedance determined the overreaching zones used in the pilot protection.

With the synchronized phasor measurement feature incorporated in some protective relays, we can obtain transmission line impedance measurements quickly and securely. With measured impedance, we can validate calculated line parameter values.

#### D. Reclosing of a Long-Line Application

A transmission line operating under a no-load condition, as shown in Fig. 25, will have an increasing voltage profile from local terminal (S) to remote terminal (R). For EHV transmission lines, the voltage at the open terminal could become excessively high [13].

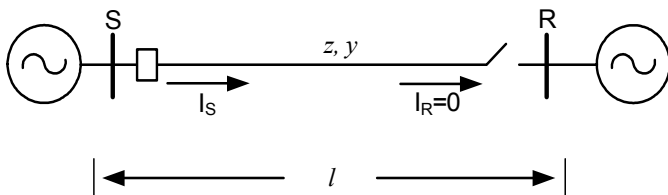


Fig. 25 Line operating with one terminal open.

The equations that relate the currents and voltages of the transmission line terminals for permanent steady-state conditions are as follows [13]:

$$V_S = V_R \cdot \cosh \gamma l + Z_C \cdot I_R \cdot \sinh \gamma l \quad (16)$$

$$I_S = Y_C \cdot V_R \cdot \sinh \gamma l + I_R \cdot \cosh \gamma l \quad (17)$$

Where:

$$Z_C - \text{Line characteristic impedance} = \sqrt{\frac{z}{y}} (\Omega)$$

$$Y_C - \text{Line characteristic admittance} = \sqrt{\frac{y}{z}} (\text{S})$$

If we assume the R terminal (Vitória) of the transmission line to be open, current  $I_R$  will be zero and Equation 16 becomes the following:

$$V_S = V_R \cdot \cosh \gamma l \quad (18)$$

Given a voltage magnitude of 1 p.u. at terminal S ( $V_S$ ), we can determine the R terminal voltage ( $V_R$ ) in terms of the line length if we know the parameters of this line. Fig. 26 shows the line voltage profile with the remote R terminal open and the S terminal voltage equal to 1 p.u. Fig. 26 uses the parameters of the Ouro Preto 2 – Vitória Transmission Line.

In the case of the nearly 400 km-long Ouro Preto 2 – Vitória line, the R terminal voltage would reach values of 1.15 p.u. for permanent steady-state conditions. This voltage value is not allowable for permanent steady-state conditions.

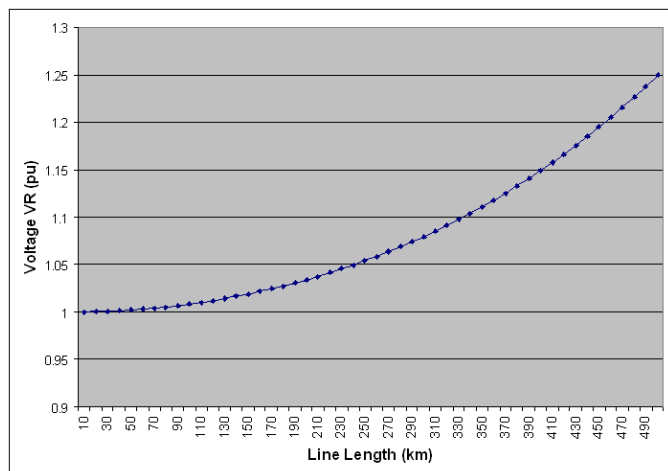


Fig. 26 Voltage profile for no-load condition.

This no-load operating condition occurs after energization or de-energization of the line from one of the terminals. To prevent the overvoltage problem that can occur after de-energization of the line from one terminal, we implemented a direct transfer trip scheme to trip the remote terminal if the local terminal trips (manual or forced trip).

By installing reactors at line ends, we prevented the overvoltage problem that occurs after line energization from one of the terminals. Through this solution, we could limit to allowed values any overvoltages resulting from line energization without load. Dedicated circuit breakers are used to switch the reactors.

During the RTDS simulation tests, we modeled the case of a single-pole trip followed by a single-pole reclose sequence

of the Ouro Preto 2 terminal, with the reactor of the Vitória terminal disconnected. This is a case of energizing the line at a no-load condition in only one phase. Fig. 27 shows the event report the Vitória terminal relay provided for this case. In this figure, the overvoltage resulting from line energization is visible and should be avoided. The simple test illustrates the type of overvoltages possible for an unloaded line and a reclosing sequence.

We implemented custom logic in the protection relay to avoid reclosing with the remote terminal reactor disconnected. This logic, as Fig. 28 illustrates, ensures that the status of the remote terminal reactor breaker supervises the local reclosing scheme.

We used relay-to-relay logic communication [4] to send the status of the reactor circuit breaker to the remote terminal. To accomplish this, the circuit-breaker auxiliary contact is an input to one of the line protection relays. We can then transmit the circuit breaker status through the communications channel to the remote terminal, as Fig. 29 illustrates. Remote terminal reclose supervision logic should include the remote reactor circuit breaker status condition in the close command circuit.

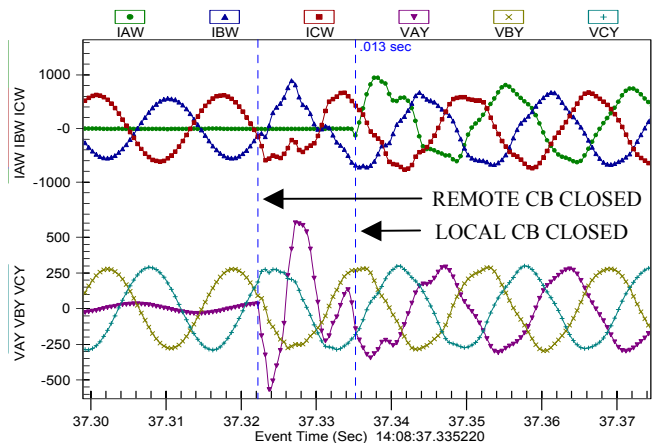


Fig. 27 Overvoltage after reclosing of the remote terminal.

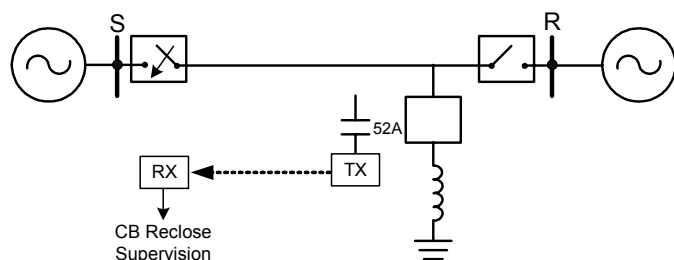


Fig. 28 Circuit breaker reclose supervision.

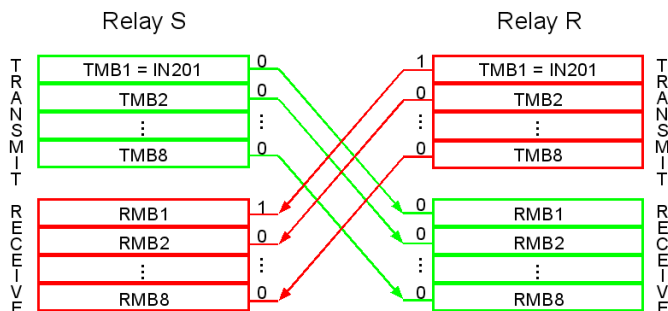


Fig. 29 Relay-to-relay logic communication.

## V. CONCLUSIONS

Modern numerical relays simplify transmission line protection and control and contribute to the customization of schemes for special needs.

The decision to adopt two totally redundant, identical (same manufacturer), and independent protection systems provides superior results, increases dependability, and facilitates design, integration, maintenance, studies, operation, and training.

Single-pole tripping schemes are advantageous in maintaining line-end substations connected by two other unfaulted phases, allowing power transfer, and reducing the possibility that the two line ends lose synchronism.

The use of the sensitive negative-sequence directional overcurrent element together with pilot protection schemes is extremely important for long lines, for which this practice increases protection system dependability.

A load-encroachment element increases the security of stepped phase distance backup protection and allows setting of the distance element to reach properly for a long transmission line.

Modern numerical relays that incorporate synchrophasor measurements allow validation of calculated impedance and line models.

A real-time digital simulator provides a comprehensive testing system to determine protection performance regarding unique protective relay applications and to validate proposed settings and logic schemes.

## VI. APPENDIX

### A. The Impedance of a Long Line

We can use Equations 19 and 20 to calculate current and voltage of a transmission line such as that shown in Fig. 30 [13]:

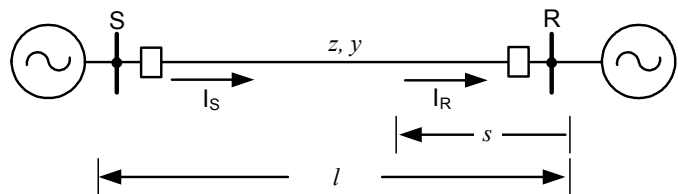


Fig. 30 Generic line.

$$V(s) = V_R \cdot \cosh \gamma s + Z_C \cdot I_R \cdot \sinh \gamma s \quad (19)$$

$$I(s) = Y_C \cdot V_R \cdot \sinh \gamma s + I_R \cdot \cosh \gamma s \quad (20)$$

To obtain the voltage and current values at the S terminal, assume  $s = l$ . We can then express voltage and current as in Equations 21 and 22:

$$V(l) = V_S = V_R \cdot \cosh \gamma l + Z_C \cdot I_R \cdot \sinh \gamma l \quad (21)$$

$$I(l) = I_S = Y_C \cdot V_R \cdot \sinh \gamma l + I_R \cdot \cosh \gamma l \quad (22)$$

### 1) Short lines

The diagram in Fig. 31 typically represents a short line [14]. For this case the line equations are the following:

$$V_S = V_R + Z \cdot I_R \quad (23)$$

$$I_S = I_R \quad (24)$$

Reference [14] provides information on how to determine if a transmission line is short, i.e., the transmission line can be considered short when maximum length of the line is:

- 60 to 80 km for lines with voltages as high as 150 kV;
- 40 km for lines from 150 kV to 400 kV;
- 20 km for lines with voltages greater than 400 kV.

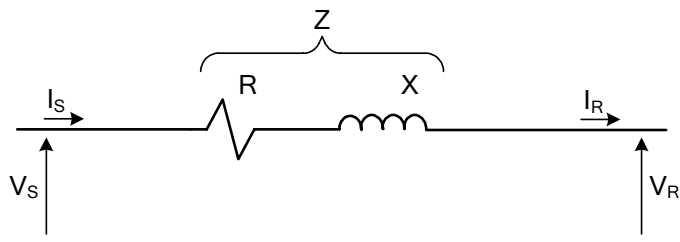


Fig. 31 Short line.

### 2) Medium Lines

Typically, the nominal  $\pi$  circuit shown in Fig. 32 represents a medium line [14].

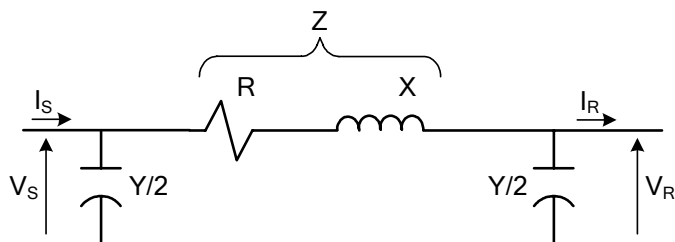


Fig. 32 Medium line.

For this case, the line equations are as follows:

$$V_S = V_R \cdot \left(1 + \frac{Z \cdot Y}{2}\right) + I_R \cdot Z \quad (25)$$

$$I_S = I_R \cdot \left(1 + \frac{Z \cdot Y}{2}\right) + V_R \cdot Y \cdot \left(1 + \frac{Z \cdot Y}{4}\right) \quad (26)$$

Line conductance is typically neglected,  $g = 0$ .

Reference [14] provides information on how to determine if a transmission line is medium, i.e., a transmission line can be considered medium when maximum line length is:

- 200 km for lines from 150 kV to 400 kV;
- 100 km for lines with voltages greater than 400 kV.

### 3) Long Lines

Long lines are those for which the calculation methods this paper presented for previous items are considered inaccurate. For long lines, we should use exact line equations (equations 21 and 22).

Considering that the equivalent  $\pi$  circuit can represent a long line, we must determine the equivalent, appropriately corrected parameters ( $Z'$  and  $Y'$ ) to gauge the effect of distributed parameters of the long transmission line.

Assuming that we can use the equivalent model shown in Fig. 33 to represent the long line, Equations 27 and 28 represent the equivalent model.

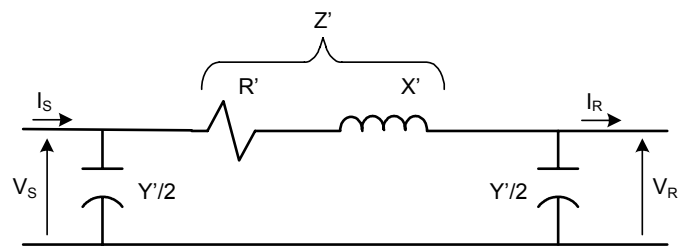


Fig. 33 Long line.

$$V_S = V_R \cdot \left(1 + \frac{Z' \cdot Y'}{2}\right) + I_R \cdot Z' \quad (27)$$

$$I_S = I_R \cdot \left(1 + \frac{Z' \cdot Y'}{2}\right) + V_R \cdot Y' \cdot \left(1 + \frac{Z' \cdot Y'}{4}\right) \quad (28)$$

Comparing equations 21 and 27, we obtain equations 29 and 30:

$$\cosh \gamma l = 1 + \frac{Z' \cdot Y'}{2} \quad (29)$$

$$Z_C \cdot \sinh \gamma l = Z' \quad (30)$$

After substituting Equation 30 in Equation 29, we obtain the following:

$$\frac{Y'}{2} = \frac{1}{Z_C} \cdot \frac{\cosh \gamma l - 1}{\sinh \gamma l} \quad (31)$$

Written another way, we can obtain the following:

$$\frac{Y'}{2} = \frac{1}{Z_C} \cdot \tanh \frac{\gamma l}{2} \quad (32)$$

From previous equations, however, we can obtain the following:

$$\frac{1}{Z_C} = \frac{1}{\sqrt{z/y}} = \frac{l \cdot \sqrt{z \cdot y}}{\sqrt{z/y} \cdot l \cdot \sqrt{z \cdot y}} = \frac{Y}{l \cdot \gamma} \quad (33)$$

After substituting Equation 33 in Equation 32, we obtain the following:

$$\frac{Y'}{2} = \frac{Y}{2} \cdot \frac{\tanh \frac{\gamma l}{2}}{\frac{\gamma l}{2}} \quad (34)$$

From Equation 30, we can then obtain the following:

$$Z' = \sqrt{z/y} \cdot \sinh \gamma l \quad (35)$$

Multiplying and dividing Equation 35 by  $1 \cdot \sqrt{z \cdot y}$ , yields the following:

$$Z' = z \cdot l \cdot \frac{\sinh \gamma l}{l \cdot \sqrt{z \cdot y}} \quad (36)$$

Or:

$$Z' = Z \cdot \frac{\sinh \gamma l}{\gamma l} \quad (37)$$

From equations 34 and 37, we can conclude that we can use the equivalent  $\pi$  circuit to represent permanent steady-state long lines. We can arrive at this conclusion because the impedance  $Z$  and the admittance  $Y$  (calculated as the product

of the values per km by the total line length) are corrected by

the factors  $\frac{\sinh \gamma l}{\gamma l}$  and  $\frac{\tanh \frac{\gamma l}{2}}{\frac{\gamma l}{2}}$ , respectively, to obtain  $Z'$  and

$Y'$ , which we can then use in the  $\pi$  transmission line model.

## VII. REFERENCES

- [1] E. O. Schweitzer, III and J. J. Kumm, "Statistical Comparison and Evaluation of Pilot Protection Schemes," in 1996 23rd Annual Western Protective Relay Conference Proceedings.
- [2] Cigré Joint Work Group 34/35.11, "Protection Using Telecommunications", December 2000.
- [3] IEEE Guide for Protective Relay Applications to Transmission Lines, IEEE Std C37.113-1999, September 1999.
- [4] K. Behrendt, "Relay to Relay Digital Logic Communication For Line Protection, Monitor and Control," in 1998 51st Annual GA Tech Protective relay Conference Proceedings.
- [5] F. Calero and D. Hou, "Practical Considerations for Single-Pole-Trip Line-Protection Schemes," in 2004 31st Western Protective Relay Conference, Spokane Proceedings.
- [6] J. L. Blackburn, "Protective Relaying: Principles and Applications," Second Edition, Marcel Dekker, Inc., New York, NY, 1998.
- [7] J. Roberts, E. O. Schweitzer, III, R. Aurora, and E. Poggi, "Limits to the Sensitivity of Ground Directional and Distance Protection," Spring Meeting of the Pennsylvania Electric Association Relay Committee, Allentown, Pennsylvania, 1997.
- [8] J. Mooney and J. Peer, "Application Guidelines for Ground Fault Protection," in 1998 51st Annual GA Tech Protective relay Conference Proceedings.
- [9] J. Roberts, A. Guzman and E. O. Schweitzer, III, "Z = V/I Does Not Make a Distance Relay," in 1993 20th Western Protective Relay Conference Proceedings.
- [10] K. Zimmerman and D. Costello, "Impedance-Based Fault Location Experience," in 2004 31st Western Protective Relay Conference Proceedings.
- [11] G. Benmouyal, A. Guzmán, E. O. Schweitzer, III, "Synchronized Phasor Measurement in Protective Relays for Protection, Control, and Analysis of Electric Power Systems," in 2002 29th Western Protective Relay Conference Proceedings.
- [12] R. Moxley, "Synchrophasors in the Real World," in 2005 Western Power Delivery Automation Conference Proceedings.
- [13] P. M. Anderson and R. G. Farmer, "Series Compensation of Power Systems," PBLSH! Inc., Encinitas, CA, 1996.
- [14] R. D. Fuchs, "Transmissão de Energia Elétrica: Linhas Aéreas; Teoria das Linhas em Regime Permanente," LTC, Rio de Janeiro, 1979.

## VIII. BIOGRAPHIES

**Ricardo Abboud**, received his BS degree in Electrical Engineering from Universidade Federal de Uberlândia, Brazil in 1992. In 1993, he started work for CPFL in Brazil. As a GTD Protection Engineer in the Protection Equipment Division, his responsibilities included maintenance, commissioning, specification, studies, and relay settings of power system protection. In 2000, he left CPFL and joined Schweitzer Engineering Laboratories as a Field Application Engineer covering the entire country of Brazil. His responsibilities include training and assisting SEL customers in substation protection and automation efforts related to generation, transmission, distribution and industrial areas. He is a member of Cigre Study Committee B5 in Brazil.

**Fernando Goldman**, received his Bachelor of Science degree in Electric Engineering from Federal University of Rio de Janeiro, Brazil in 1979. He started working for Berenhauser Engineering and Consulting in 1978 as a trainee and worked there after 1979 as an engineer. Since 1979, he has specialized in substation and power plant system protection. He joined Furnas Centrais Elétricas S.A. in 1981, at Nuclear Power Plant of Angra dos Reis. In 1986, he joined the Electric Engineering Department at Furnas, and he has

been proactively involved in the design, management, and modernization of several substations in the Furnas transmission system. In 2005, he moved to the Furnas Transmission Training Center.

**Walmer Ferreira Soares**, received his Bachelor of Science degree in Electrical Engineering from Santa Úrsula University in 1992 and his post-graduate degree in protection systems from Rio de Janeiro Federal University in 2003. He joined Furnas Centrais Elétricas S.A. in 1993 and specializes in protection systems. He is involved in studies, tests in RTDS, commissioning of protection systems, and disturbance analysis.